

## Measurement system configuration for damage identification of continuously monitored structures

Irwanda Laory<sup>a</sup>, Nizar Bel Hadj Ali<sup>b</sup>, Thanh N. Trinh<sup>a</sup>, Ian F. C. Smith<sup>a</sup>

<sup>a</sup>Swiss Federal Institute of Technology Lausanne (EPFL), Station 18, CH-1015 Lausanne, Switzerland

<sup>b</sup>Ecole Polytechnique de Tunisie, University of Carthage, B.P. 743, La Marsa 2078, Tunisia

1

### 2 **Abstract**

3

4 Measurement system configuration is an important task in structural health monitoring in that  
5 decisions influence the performance of monitoring systems. This task is generally performed using  
6 only engineering judgment and experience. Such approach may result in either a large amount of  
7 redundant data and high data-interpretation costs, or insufficient data leading to ambiguous  
8 interpretations. This paper presents a systematic approach to configure measurement systems  
9 where static measurement data are interpreted for damage detection using model-free (non-physics-  
10 based) methods. The proposed approach provides decision support for two tasks: (1) determining  
11 the appropriate number of sensors to be employed and (2) placing the sensors at the most  
12 informative locations. The first task involves evaluating the performance of measurement systems in  
13 terms of the number of sensors. Using a given number of sensors, the second task involves  
14 configuring a measurement system by identifying the most informative sensor locations. The  
15 locations are identified based on three criteria: the number of non-detectable damage scenarios, the  
16 average time to detection and the damage detectability. A multi-objective optimization is thus  
17 carried out leading to a set of non-dominated solutions. To select the best compromise solution in  
18 this set, two multi criteria decision making methods, Pareto-Edgeworth-Grierson multi-criteria  
19 decision making (PEG-MCDM) and Preference Ranking Organization METHod for Enrichment  
20 Evaluation (PROMETHEE), are employed. A railway truss bridge in Zangenberg (Germany) is used as a  
21 case study to illustrate the applicability of the proposed approach. Measurement systems are

22 configured for situations where measurement data are interpreted using two model-free methods:  
23 Moving Principal Component Analysis (MPCA) and Robust Regression Analysis (RRA). Results  
24 demonstrate that the proposed approach is able to provide engineers with decision support for  
25 configuring measurement systems based on the data-interpretation methods used for damage  
26 detection. The approach is also able to accommodate the simultaneous use of several model-free  
27 data-interpretation methods. It is also concluded that the number of non-detectable scenarios, the  
28 average time to detection and the damage detectability are useful metrics for evaluating the  
29 performance of measurement systems when data are interpreted using model-free methods.

30 **Subject headings:** Bridges; damage; monitoring; measurement; optimization; decision making

31 **Keywords:** Measurement system configuration; model-free data interpretation; damage  
32 detectability; multi-objective optimization; multi-criteria decision-making

## 33 **Introduction**

34 Recent advances in sensor technology and data acquisition systems enable engineers to continuously  
35 monitor civil engineering infrastructures so that damage can be detected before it reaches a critical  
36 level. Many structures have been monitored using sophisticated measurement systems with a large  
37 number of sensors. The cable-stayed Stonecutters Bridge in Hong Kong, for example, is equipped  
38 with more than 1200 sensors, including accelerometers, temperature sensors, strain gauges and  
39 other sensors (Ni et al. 2008). In many cases, due to the lack of systematic approaches for the  
40 configuration of measurement systems, the number of sensors and their locations were determined  
41 using engineering judgement alone. This approach may result either in a large amount of redundant  
42 data or insufficient data. Redundant data leads to high data-interpretation costs while insufficient  
43 data results in ambiguous interpretations. Therefore, a systematic approach for measurement  
44 system configurations that provide good performance for damage identification is desirable.

45 Damage in civil structures may be identified by interpreting monitoring data collected using  
46 measurement systems. The task of measurement interpretation falls into the broad area of system

47 identification. There are generally two classes of data-interpretation methods in system  
48 identification: model-based (physics-based) methods and model-free (non-physics-based) methods  
49 (ASCE 2011). Model-based data-interpretation methods typically utilize measurement data to  
50 identify models that are able to predict the real behaviour of structures (Aref et al. 2005; Chen and  
51 Wu 2010; Jaishi and Ren 2006; Koh and Thanh 2009; Robert-Nicoud et al. 2005a). However, for civil  
52 infrastructure, creating such models is often difficult, expensive and may not reflect the real  
53 structural behaviour because of the uncertainties that are common in complex civil-engineering  
54 structures (Goulet et al. 2010). Furthermore, model-based methods are not necessarily successful in  
55 identifying structural behavior (Saitta et al. 2005).

56 Model-free data-interpretation methods, on the other hand, involve interpreting measurement data  
57 without geometrical and material information (i.e. without structural models). These methods  
58 identify damage by tracking changes in time-series signals; thus, they are well-suited for interpreting  
59 measurements during continuous monitoring of structures. Liu et al. (2009) developed a limit state  
60 equation for safety evaluation of existing bridges. Hou et al. (2000) proposed a wavelet-based  
61 approach for structural damage detection. Omenzetter and Brownjohn (2006) proposed an  
62 autoregressive integrated moving average model method for damage detection. Lanata and Grosso  
63 (2006) applied a proper orthogonal decomposition method for continuous static monitoring of  
64 structures. Yan et al. (2005) proposed local PCA-based damage detection for vibration-based  
65 structural health monitoring. Posenato et al. (2010; 2008) proposed two model-free data-  
66 interpretation methods: (1) Moving Principal Component Analysis (MPCA) and (2) Robust Regression  
67 Analysis (RRA), to detect and localize damage in civil engineering structures. These two methods  
68 were compared with many other methods and it was demonstrated that their performance for  
69 damage detection was superior to the other methods when dealing with civil-engineering challenges  
70 that include high noise, missing data and outliers.

71 Configuration of measurement systems is based on the methods that are used to interpret  
72 measurement data (i.e. different methods may result in different measurement configurations).

73 Thus, in order to maximize the performance of measurement systems, data-interpretation methods  
74 should be selected prior to configuration task. Previous studies (Kang et al. 2008; Li et al. 2007; Li et  
75 al. 2004; Liu et al. 2008; Meo and Zumpano 2005; Papadimitriou 2004) have mainly focused on the  
76 configuration of measurement systems for dynamic tests where measurement data is interpreted  
77 using model-based methods. Li et al. (2007) investigated and compared two measurement system  
78 configuration methods, modal kinetic energy and effective independence, for damage identification  
79 using dynamic tests. Kang et al. (2008) proposed a virus co-evolutionary partheno-genetic algorithm,  
80 which combined a partheno-genetic algorithm with virus evolutionary theory, to place sensors on a  
81 large space structure for the purpose of modal identification. Meo and Zumpano (2005) investigated  
82 six different measurement system configuration techniques for optimum identification of structural  
83 vibration characteristics. For multiple-model methods using static measurements, Robert-Nicoud et  
84 al. (2005b) proposed an iterative greedy algorithm to design a measurement system that gives  
85 maximum separation between predictions of candidate models. Kripakaran and Smith (2009) utilized  
86 damage scenario generation and proposed strategies for two measurement tasks: (1) configuring  
87 initial measurement systems and (2) enhancing these systems for subsequent measurements once  
88 data interpretation is carried out. Few studies have used damage scenario generation as a starting  
89 point for measurement system configuration. Although many studies have been performed to  
90 design measurement systems for structural identification, none have studied the measurement  
91 system configuration for model-free data-interpretation methods using static measurements.

92 The number of potential configurations for a measurement system is exponentially related to the  
93 number of possible sensor locations (Saitta et al. 2006). Hence, the task of configuring measurement  
94 systems is best carried out using global search algorithms. In several studies (Kripakaran and Smith  
95 2009; Liu et al. 2008; Rakesh and et al. 2008; Rao and Ganesh 2007; Tongpadungrod et al. 2003;  
96 Wang et al. 2002; Xu et al. 2010), stochastic search techniques were employed for measurement  
97 system configuration. The evaluation of the potential configurations should include several criteria  
98 (objectives). For example, good configurations have a minimum number of sensors with a maximum

99 performance. For optimizing placements of active control devices and sensors, Cha et al. (2011)  
100 proposed a methodology that minimizes the number of employed devices and sensors while  
101 maximizing structural performance under earthquake. In most cases, objectives are non-  
102 commensurable (i.e. they are measured in different units) and usually in conflict with each other.  
103 There may be no solution satisfying all objectives simultaneously. Thus, the solution is often a set of  
104 non-dominated solutions (Pareto-optimal solutions), or a compromise solution according to  
105 engineers' preferences.

106 The task of selecting a compromise solution falls into the field of multi-criteria-decision-making  
107 (MCDM). Grierson (2008) proposed Pareto-Edgeworth-Grierson multi-criteria decision-making (PEG-  
108 MCDM) that employs a trade-off-analysis technique to identify compromise solutions for which the  
109 competing criteria are mutually satisfied in a Pareto-optimal sense. The PEG-MCDM procedure can  
110 be effectively applied to MCDM tasks that involve many objectives and feasible solutions. Another  
111 method for MCDM is Preference Ranking Organization METHod for Enrichment Evaluation  
112 (PROMETHEE) (Behzadian et al. 2010; Brans and Mareschal 2005a; Brans 1982; Brans et al. 1986).  
113 This method utilizes a preference index to compute a net flow for each Pareto optimal solution. This  
114 value is then used to rank the Pareto optimal set. Bel Hadj Ali and Smith (2010) compared PEG-  
115 MCDM and PROMETHEE for vibration control of a tensegrity structure.

116 This paper presents a systematic method-based approach to configure measurement systems where  
117 static measurement data are interpreted using model-free (non-physic-based) methods. The  
118 approach involves damage scenario generation, optimization of several criteria and multi-criteria  
119 decision-making. It consists of two steps. The first step is to provide decision support for engineers  
120 to determine the number of sensors to be employed. The second step is to configure sensor  
121 locations based on three criteria: the number of non-detectable scenarios, damage detectability and  
122 the average time to detection. A genetic algorithm (Sastry 2007) is employed to evaluate potential  
123 configurations based on a multi-objective optimization. Then, two multi-criteria decision-making  
124 methods, PEG-MCDM and PROMETHEE, are applied to provide support for identifying the best

125 compromise configuration. To illustrate the performance of the proposed approach, measurement  
126 systems are configured for the Zangenberg railway bridge in Germany, where the measurement data  
127 are interpreted using Moving Principal Component Analysis and Robust Regression Analysis.

## 128 **Model-free (non-physics-based) data-interpretation methods**

### 129 **Moving principal component analysis (MPCA)**

130 MPCA is a modified version of principal component analysis (PCA) (Hubert et al. 2005). PCA is a  
131 mathematical process of transforming a number of possibly correlated variables into a smaller  
132 number of uncorrelated variables, called principal components. The first few components retain  
133 most of the variation present in the original variables. In the context of structural health monitoring,  
134 PCA is employed to enhance the discrimination between features of undamaged and damaged  
135 structures and to reduce computational time. Posenato et al. (2008) proposed “moving” PCA (MPCA)  
136 that essentially applies PCA to a moving constant-sized window of measurements instead of the  
137 whole dataset. MPCA is applied to measurement time histories by first constructing a matrix that  
138 contains the history of all the measured parameters and second iteratively extracting datasets  
139 corresponding to a moving window and computing the principal components using PCA.

140 The principal components are the eigenvectors of the covariance matrix of extracted measurements.  
141 Sorting the eigenvectors by eigenvalues in decreasing order, the components are arranged in order  
142 of significance. The first few principal components contain most of the variance of the time series  
143 while the remaining components are defined by measurement noise. Thus, MPCA is carried out by  
144 analyzing only the eigenvectors that are related to the first few eigenvalues. When damage occurs,  
145 mean values and components of the covariance matrix change and as consequence, so do values of  
146 eigenvalues and eigenvectors. An advantage of using a moving window rather than whole  
147 measurements is less computational time and earlier damage detection since very old measurements  
148 do not bias results. Another advantage is adaptability. Once new behaviour is identified, adaptation  
149 enables detection of further damage.

## 150 **Robust regression analysis (RRA)**

151 Robust regression analysis (Andersen 2008; Jajo 2005) involves assigning a weight to each data point  
152 using a process called iteratively reweighted least squares. This method achieves more reliable  
153 results than linear regression analysis when measurement data are subjected to outliers. RRA is  
154 applied for continuous monitoring of structures by finding all sensor pairs that have a high  
155 correlation and then to focus on the correlation of these couples to detect anomalies. To find sensor  
156 pairs with a high correlation, the correlation coefficients  $r_{s_i, s_j}$  between measurements from two  
157 sensors  $s_i$  and  $s_j$  are computed and compared with the correlation coefficient threshold that is  
158 chosen to be 0.8 in this study. All sensor pairs having a correlation coefficient greater than the  
159 threshold are selected in order to formulate the robust regression model. The linear relation  
160 between  $s_i$  and  $s_j$  is written as

$$161 \quad s'_j = as_i + b \quad (1)$$

162 where  $s'_j$  represents the value of  $s_j$  computed according to the linear relation.  $a$  and  $b$  are the  
163 coefficients of the robust regression line estimated from measurements. These coefficients are  
164 estimated using iteratively reweighted least squares. The robust regression analysis is carried out by  
165 observing the difference between the measurements  $s_j$  and the prediction by linear regression-line  
166  $s'_j$ , called regression residuals. Standard deviation of the residuals is used to define the threshold of  
167 confidence intervals for each pair. Damage is identified when the value exceeds the confidence  
168 interval. In addition to the advantage of being insensitive to outliers and missing data, RRA is capable  
169 of adapting to the new state of a structure and thus permitting the identification of further  
170 anomalies.

## 171 **Task formulation and optimization**

172 Measurement system configuration involves placing sensors at the most informative locations such  
173 that the performance of damage detection is maximized. The number of sensors to be placed and

174 potential sensor locations leads to a space of possible measurement system configurations. Even  
175 with a small number of possible sensor locations, it is practically impossible to generate and test all  
176 configurations due to the combinatorial nature of the task. Deterministic optimization methods, for  
177 example “branch and bound” may be able to treat small combinatorial tasks. However, evaluating all  
178 combinations of  $i$  sensors among  $n$  possible locations has the following computational complexity:

$$179 \sum_{i=1}^n C_n^i = 2^n - 1 \quad (2)$$

180 Stochastic search is particularly useful in such situation. Stochastic methods support search well in  
181 complex and large solution spaces. Although there is no guarantee of reaching a global optimum,  
182 near optimal solutions are usually obtained.

183 In this paper, three objective functions are used to evaluate a configuration of sensor placements  
184 represented by a vector of  $N$  decision variables  $\mathbf{x}^t = [x_1, x_2, \dots, x_N]$ . The first objective function  $f_1$  is  
185 to evaluate the number of non-detectable damage scenarios for a measurement configuration. The  
186 second objective function  $f_2$  is to evaluate the damage detectability which is defined through the  
187 average of the minimum detectable damage level using MPCA and RRA as follows:

$$188 \text{Damage detectability (\%)} = 100\% - \text{Minimum detectable damage level (\%)} \quad (3)$$

189 where the minimum detectable damage level is the smallest percentage loss of member-stiffness  
190 that can be detected. The third objective function  $f_3$  is to evaluate the average time-to-detection  
191 associated with a measurement configuration. Time-to-detection is the period (in days) from the  
192 moment damage occurs in the structure to the moment damage is detected. The value of  $f_3$  is  
193 obtained by averaging the time-to-detection for the whole set of detected damage scenarios.

194 From these three objective functions, measurement system configuration is formulated as a multi-  
195 objective optimization task that results in a set of possible solutions. Solutions are known as Pareto  
196 optimal (non-dominated) solutions. In a multi-objective minimization task, a solution is called Pareto

197 optimal if there is no other solution that satisfies one objective function more without having a  
198 worse value for at least one other objective function. Many evolutionary multi-objective optimization  
199 methods have been used in various fields due to their effectiveness and robustness in searching for a  
200 set of trade-off solutions (Coello Coello et al. 2007). In this study, measurement system  
201 configurations are represented by a finite number of discrete variables. Two stochastic search  
202 algorithms are tested for this task: Probabilistic Global Search Lausanne (PGSL) (Raphael and Smith  
203 2003) and Genetic Algorithms (GA) (Sastry 2007). The genetic algorithm is finally adopted for the  
204 multi-objective optimization task where optimization variables are coded as integer strings.

## 205 **Multi-criteria decision making**

206 In order to identify a good solution among the set of the Pareto optimum solutions for configuring a  
207 measurement system, our approach employs two Multi-Criteria Decision Making (MCDM) methods:  
208 Preference Ranking Organization METHod for Enrichment Evaluation (PROMETHEE) (Brans and  
209 Mareschal 2005a; Brans 1982; Brans et al. 1986) and Pareto-Edgeworth-Grierson multi-criteria  
210 decision making (PEG-MCDM) (Grierson 2008).

### 211 **Preference Ranking Organization METHod for Enrichment Evaluation (PROMETHEE)**

212 The PROMETHEE method was developed as a MCDM method to solve discrete decision tasks with  
213 conflicting criteria to establish ranking of Pareto-optimal solutions with conflicting criteria.  
214 Incorporating preferences is also considered to help to handle conflicting objectives (Fleming et al.  
215 2005). An aggregated preference index is used to compute outranking flows for each Pareto optimal  
216 solution. These outranking flows are then exploited to establish a *partial* ranking (PROMETHEE I) or a  
217 *complete* ranking (PROMETHEE II) on the Pareto set.

218 Let  $s_1, \dots, s_n$  be  $n$  Pareto optimal solutions and  $f_1, \dots, f_m$  denote the  $m$  decision criteria for PROMETHEE  
219 I., The PROMETHEE procedure is based on pairwise comparisons between Pareto optimal solutions.  
220 This method assumes that the preference between two solutions for a given criterion can be  
221 expressed using ratios. Brans and Mareschal (2005b) proposed six types of preference functions

222  $P_k(S_i, S_j)$  used to express the magnitude of the preference between two solutions  $S_i$  and  $S_j$  on  
 223 the criterion  $k$  by a real value in the interval  $[0, 1]$ . Using preference functions associated with all  
 224 decision criteria, an aggregate preference index  $C(S_i, S_j)$  is thus defined in Eq.(4) , where  $w_k$  are  
 225 weights expressing the relative preference of the decision criteria.

$$226 \quad C(S_i, S_j) = \frac{\sum_{k=1}^m w_k \cdot P_k(S_i, S_j)}{\sum_{k=1}^m w_k} \quad (4)$$

227 Once the aggregate preference indexes are computed for each pair of the Pareto solutions,  
 228 outranking flows can be evaluated. The preference flows ( $\varphi^+$ ,  $\varphi^-$  and  $\varphi$ ) for each solution are  
 229 formulated as follows:

$$230 \quad \varphi^+(S_i) = \sum_{j=1}^n C(S_i, S_j) \quad (5)$$

$$231 \quad \varphi^-(S_i) = \sum_{j=1}^n C(S_j, S_i) \quad (6)$$

$$232 \quad \varphi(S_i) = \varphi^+(S_i) - \varphi^-(S_i) \quad (7)$$

233 The positive flow ( $\varphi^+(S_i)$ ) expresses the intensity of preference of the solution  $S_i$  over all other  
 234 solutions in the solution set. The negative flow ( $\varphi^-(S_i)$ ) expresses the intensity of preference of all  
 235 other solutions over solution  $S_i$ . The difference between the positive and the negative flow gives the  
 236 net preference flow ( $\varphi(S_i)$ ), which is the absolute preference of the solution  $S_i$  over all other  
 237 solutions in the solution set. For PROMETHEE II, this value is used to establish a complete ranking of  
 238 all Pareto optimal solutions.

### 239 **Pareto-Edgeworth-Grierson multi-criteria decision making (PEG-MCDM)**

240 Grierson (2008) proposed a MCDM strategy employing a trade-off-analysis technique to identify  
 241 compromise solutions for which the competing criteria are mutually satisfied in a Pareto optimal set.  
 242 Grierson (2008) formulated the PEG-theorem which states existence and uniqueness of a Pareto-  
 243 compromise solution that represents a mutually agreeable trade-off between conflicting criteria for

244 multi-objective optimization tasks. The PEG-MCDM method is summarized here for the case of a  
 245 two-criteria decision task. Refer to (Grierson 2008) for detailed description of a general case.

246 Having the Pareto-optimal set of solutions from a multi-objective optimization, let  $f_1, \dots, f_n$  denote  
 247 the  $n$  vectors that define the Pareto-optimal data constituted by  $m$  Pareto-optimal solutions. The  
 248 original Pareto data are first normalized to find  $m$ -dimensional vectors  $\mathbf{x}_i$ .

$$249 \quad x_i = \frac{f_i - f_i^{\min}}{f_i^{\max} - f_i^{\min}}; \quad (i = 1, n) \quad (8)$$

250 The  $m$  entries of each of the  $n$  vectors are sequentially reordered from their minimum to maximum.  
 251 For  $n = 2$  decision criteria, the Pareto data are thus represented by two  $m$ -dimensional normalized  
 252 vectors.

$$253 \quad \mathbf{x}_1^T = [x_1^{\min}, \dots, x_1^{\max}] \text{ and } \mathbf{x}_2^T = [x_2^{\max}, \dots, x_2^{\min}] \quad (9)$$

254 In order to obtain a competitive equilibrium state at which a Pareto trade-off can take place between  
 255 the two criteria, Grierson (2008) proposed an approach for transforming the Pareto data without  
 256 changing its ordinal character so that a unique Pareto trade-off between two criteria is mutually  
 257 agreeable. This is done by transforming the normalized Pareto curve to a circular Pareto that has only  
 258 one competitive equilibrium state. In order to perform this transformation analytically, the criteria  
 259 vectors  $\mathbf{x}_1$  and  $\mathbf{x}_2$  are uniformly shifted and then re-normalized to obtain vectors  $\mathbf{x}_1^*$  and  $\mathbf{x}_2^*$

$$260 \quad \mathbf{x}_i^* = (\mathbf{x}_i - \delta \mathbf{x}_i) / (1 - \delta x_i) \quad (i = 1, 2); \quad \delta x_1 = \delta x_2 = \sqrt{2} - 1 \quad (10)$$

261 The objective criteria values corresponding to the unique competitive equilibrium point are  
 262 evaluated.

$$263 \quad f_i^0 = f_i^{\max} - (f_i^{\max} - f_i^{\min}) (\Delta r_0 + \sqrt{2}/2); \quad (i = 1, 2) \quad (11)$$

264 where  $f_i^0$  is the value of the two objective functions for the Pareto-compromise solution.  $\Delta r_0$  is the  
 265 radial shift from the transformed Pareto curve to the unique competitive equilibrium point. A ranking  
 266 of the original Pareto data set may be achieved by computing the distance of the Pareto solutions to

267 the Pareto-compromise solution. This distance is represented by the mean-square-error between the  
268 criteria values  $f_i^0$  for the Pareto-compromise solution and the corresponding criteria values  $f_i$  for  
269 each of the  $m$  original Pareto solutions.

## 270 **Measurement system configuration**

271 The aim of measurement system configuration is to enhance the effectiveness of data-interpretation  
272 tasks for monitoring of structures. Therefore, the performance of a measurement configuration is  
273 evaluated based on criteria associated with damage-detection capacity of data-interpretation  
274 methods. The proposed approach involves damage scenario generation, multi-objective optimization  
275 and multi-criteria decision-making. Damage scenarios depend upon structural factors such as  
276 material, geometry, structural characteristics and geographical location. These scenarios can be  
277 represented by the value of structural parameters which are specified by engineer. For example,  
278 damage in a structural element may be modelled as the percentage reduction in axial or flexural  
279 stiffness. Damage scenarios are employed as benchmark situations to evaluate the performance of a  
280 given measurement system.

281 As described in the task formulation section (section 3), measurement configuration involves multi-  
282 objective optimization task considering several criteria. Multi-objective optimization can lead to  
283 solutions with the minimal number of sensors and optimal placements in one step. However, in  
284 practical situations, measurement system configuration is often a weakly defined task where there  
285 are criteria that are not explicitly taken into account. Such criteria may include access for installation,  
286 additional measurement needs and sensor maintenance cost. In such situations, support tools that  
287 enable decision makers to be involved in the process are preferable. Therefore, instead of providing  
288 decision makers with optimal solutions according to incomplete criteria, explicit trade-off  
289 information is provided for the number of sensors versus performance in the first step.

290 In order to obtain information about the trade-off, multi-objective optimization and multi-criteria  
291 decision-making need to be performed iteratively for increasing number of sensors. The  
292 computational complexity (using O notation) of such a task is as follows

$$293 \quad C_{total} = (C_1 \cdot n_1 \cdot n_2 + C_2) \cdot n_3 \quad (12)$$

294 where  $C_{total}$  is the total complexity of the task,  $C_1$  is the complexity of data-interpretation method,  
295  $n_1$  is the number of damage scenarios,  $n_2$  is the number of evaluations that is required to converge  
296 to the optimal solutions,  $C_2$  is the complexity of the multi-criteria decision-making method and  $n_3$  is  
297 the number of incremental steps when increasing the number of sensors. Eq.11 shows that the  
298 number of damage scenarios and evaluations are linearly proportional to the total complexity of the  
299 task. The number of damage scenarios and evaluations that are required for multi-objective  
300 optimization are higher than that for single-objective optimization. Multi-objective optimization can  
301 be carried out by transforming additional criteria into constraints in a single-objective optimization.  
302 The number of evaluations for such approach ( $n_{total}$ ) is the upper bound of the number of evaluations  
303 in multi-objective optimization as follows

$$304 \quad n_{total} = n_s \cdot (P)^{m-1} \quad (13)$$

305 where  $n_s$  is the number of evaluations for a single-objective optimization,  $P$  is the number of  
306 Pareto-points corresponding to an additional objective and  $m$  is the number of objectives. Eq.12  
307 shows that the total number of evaluations is exponentially related to the number of objectives. For  
308 example, assuming  $n_s = 400$  and  $P = 10$ , the number of evaluations increases from 400 to 40000  
309 when the number of objectives increases from 1 to 3. The time required for an evaluation depends  
310 on factors such as algorithms that are used for data interpretation, the size of data and the computer  
311 system that is used to perform the task. For the situation that is studied in this paper, the  
312 computational time for one evaluation took about 5 seconds. Table 1 shows the results of the  
313 execution-time estimations for this example where the time to perform one evaluation is assumed to

314 be 5 seconds. In comparison with single-objective optimization, performing multi-objective  
315 optimization leads to much higher computational costs. Furthermore, when the solution space  
316 becomes too large, performing multi-objective optimization is no-longer likely to obtain near optimal  
317 solutions.

318 Considering that not all information can be accounted for explicitly as well as the computational  
319 complexity associated with increasing number of objectives, measurement system configuration is  
320 carried out in two steps.

- 321 • A preliminary step using single-objective optimization to explore solution space in order to  
322 decide on the appropriate number of sensors to be employed
- 323 • A in-depth search step using multi-objective optimization in order to provide decision  
324 support to place sensors at the most informative locations

325 The two-step procedure for measurement system configuration is illustrated in Figure 1. In the first  
326 step, the solution space is explored by minimizing the number of non-detectable damage scenarios  
327 and by observing the improvement of the measurement system performance with respect to the  
328 increasing number of sensors. Engineers are thus able to determine the appropriate number of  
329 sensors through identifying where the addition of sensors will not give a significant improvement in  
330 performance.

331 Given the number of sensors to be employed, the second step is to configure measurement systems  
332 by identifying the best sensor locations. After the first step of preliminary exploration, this step  
333 conducts an in-depth exploration in a narrower solution space for measurement configurations.  
334 Performance is evaluated using all three specific criteria: minimizing the number of non-detectable  
335 scenarios, maximizing the damage detectability and minimizing the average time to detection. Multi-  
336 objective optimization using GA is carried out to identify sensor locations for measurement system  
337 that offers the best performance based on the specified criteria. Since all criteria are considered in  
338 this step, multi-objective optimization yields a set of non-dominated solutions (Pareto-optimal

339 solutions). Therefore, MCDM methods (PEG-MCDM and PROMETHEE) are adopted to provide  
340 decision support for selecting the best compromise solution.

## 341 **Case study**

342 To illustrate the performance of the approach for measurement system configuration, a railway truss  
343 bridge in Zangenberg, Germany has been selected. This 80-m steel bridge is composed of two parallel  
344 trusses each having 77 members. Their properties are summarized in Table 2. The truss members  
345 are made of steel having an elastic modulus of 200 GPa and a density of 7870 kg/m<sup>3</sup>. A finite  
346 element analysis that includes traffic loading and temperature variation provides responses (strains)  
347 that are taken as the measurement from continuous monitoring. Traffic loading is simulated by  
348 applying a randomly generated vertical load (0-19 tonnes) at each node in the bottom chords. A load  
349 of 19 tonnes is equivalent to an axle load of a railway locomotive. Daily and seasonal variations are  
350 simulated as temperature loads. Temperature differences between top and bottom chords due to  
351 solar radiation are also taken into account in the simulations.

352 One truss of the bridge fixed at both ends is modelled (Figure 2). Although this is not the boundary  
353 conditions that were designed for the bridge, two fixed ends represent the upper-bound worst case  
354 for supports that have deteriorated with age. Damage scenarios are generated where each scenario  
355 represents axial-stiffness reduction of a member. Potential configurations are evaluated based on  
356 the performance of detecting these damage scenarios. Two data-interpretation methods (MPCA and  
357 RRA) for damage detection are adopted in this study.

358 In the first step, a global search is used to estimate the maximum performance of configurations in  
359 terms of the increasing number of sensors. For every number of sensors, the maximum performance  
360 is estimated by minimizing the number of non-detectable scenarios. Seventy-seven damage  
361 scenarios are generated where each scenario represents 50% axial stiffness reduction of a member.  
362 The results of the first step for both MPCA and RRA are shown in Figure 3. It is demonstrated that  
363 MPCA can detect more scenarios than RRA. For both methods, the number of non-detectable

364 damage scenarios initially reduces rapidly when the number of sensors increases. However, the  
365 reduction tapers off and the improvement of the performance becomes marginal when the number  
366 of sensors is greater than 24. For MPCA, the number of non-detectable scenarios decreases from 45  
367 to 15 when the number of sensors is increased from 4 to 24. Adding more sensors can only decrease  
368 the non-detectable scenario by 15 scenarios. For RRA, a reduction of 27 non-detectable scenarios is  
369 gained by adding the sensors from 4 to 24. Increasing the number of sensors from 24 to 77 only  
370 reduced the number of non-detectable scenarios by 12 scenarios. These results show that adding  
371 more sensors will only result in small improvement of the system performance. Therefore, 24  
372 sensors are decided for this measurement system.

373 Given the number of sensors to be employed, the measurement system is configured using a multi-  
374 objective optimization procedure and MCDM approaches. In the multi-objective optimization  
375 procedure, objective functions are minimizing the number of non-detectable scenarios, maximizing  
376 the damage detectability and minimizing the average time to detection. Figure 4 and 5 show the  
377 pareto-optimal solutions for both MPCA and RRA. Time to detection for RRA is much smaller than  
378 that of MPCA. On the other hand, MPCA is able to detect more damage scenarios and has higher  
379 detectability than RRA. These results indicate that RRA is able to detect damage faster than MPCA  
380 but MPCA is better in terms of damage detectability. The Pareto-optimal solutions are then ranked  
381 using PEG-MCDM and PROMETHEE. Table 3 and 4 show the ranks of the Pareto-optimal solutions for  
382 MPCA and RRA respectively. While PROMETHEE ranks the solutions based on the preference flow,  
383  $\varphi$ , ranking in PEG-MCDM is based on the distance of the solution to the Pareto-compromise  
384 solution. Preference flow,  $\varphi (S_i)$ , is the absolute preference of the solution  $S_i$  over all other  
385 solutions in the solution set. Distance represents the proximity of the solution to the Pareto-  
386 compromise solution that is mutually agreeable for all objectives. For MPCA, employing the PEG-  
387 MCDM procedure, the Pareto-compromise solution mutually agreeable for all objectives is a  
388 configuration with the value of criteria 1 = 18.5, that of criteria 2 = 120.6 and that of criteria 3 = 14.2.  
389 The closest solution to this is configuration 7 as shown in Table 3. This configuration is however

390 ranked as the 3<sup>rd</sup> place when PROMETHEE is used for outranking. On the other hand, the best  
391 configuration (number 8) from PROMETHEE is ranked as the 2<sup>nd</sup> place when using PEG-MCDM. For  
392 RRA, while the best-compromise configuration (number 13) from PEG-MCDM is ranked 4<sup>th</sup> in the  
393 results when using PROMETHEE, the best-compromise configuration (number 16) from PROMETHEE  
394 is ranked in 2<sup>nd</sup> when using PEG-MCDM. These results show that the best compromise configuration  
395 defined by using PROMETHEE and PEG-MCDM are different. This demonstrates that a compromise  
396 solution with mutually agreeable objectives is not necessarily the preferred solution using  
397 preference-based outranking strategy.

398 For situations where information related to the relative preference of criteria is not available or  
399 limited, it is preferable to employ PEG-MCDM method since it provides a solution that mutually  
400 satisfies all criteria. On the other hand, when preferences information is available and it is possible to  
401 build mathematical models of them, PROMETHEE is a better option. This method provides the best  
402 compromise solution based on various preference forms. Results indicate that multi-criteria  
403 decision-making methods are capable of providing support for selecting the best compromise-  
404 measurement system.

405 In order to take advantages of many data-interpretation methods, engineers may decide to employ  
406 simultaneously several model-free data-interpretation methods. For such situations, a compromise  
407 solution which accommodates several methods is desirable. A solution for this can be obtained in  
408 two ways. The first is by configuring optimal measurement-system for each method and taking the  
409 union of these optimal configurations as the best compromise solution. However, this may result in  
410 excessive number of sensors. For this case study, a union of best compromise configuration for  
411 MPCA and RRA results in 38 sensors. Alternatively, a compromise solution can be obtained by  
412 treating several methods as a combined method and performing configuration based on the  
413 evaluation of the combined performance for each potential configuration. This case is referred to as  
414 optimized combination.

415 Figure 6 shows respectively the optimum configurations resulting from use of MPCA, RRA, the union  
416 of these solutions and the optimized combination. Mid-span, bottom chord is one of the most  
417 common locations for sensors that is often intuitively selected by engineers. As shown in the figure,  
418 no sensor is placed in this location. This demonstrates that the methodology uncovers solutions that  
419 would not have been found using engineering judgment alone. For MPCA, no sensor is placed at  
420 bottom chord while sensors are mainly distributed at the bottom chord for RRA. The results  
421 demonstrate that different methods result in different measurement configurations.

422 Table 5 shows the performance of the best compromise measurement configuration for MPCA, RRA  
423 and their combinations using three criteria. The performance of the measurement systems in the  
424 case of an optimized combination (24 sensors) is better than that of a direct combination (38  
425 sensors). As compared with MPCA, a direct combination of optimum configurations for MPCA and  
426 RRA only improves the performance in terms of time to detection. This is because such combination  
427 places additional sensors at non-informative places. On the other hand, a better performance in all  
428 three criteria is shown for the case of an optimized combination. These results demonstrate that the  
429 proposed approach is able to combine results of various model-free data-interpretation methods.  
430 Finally, engineers may uncover non-intuitive solutions using the approach described in this paper.

## 431 **Conclusions**

432 The following conclusions are drawn from this research.

- 433 • The proposed approach for measurement system configuration is able to accommodate  
434 model-free (non-physics-based) data interpretation methods for damage detection of  
435 continuously monitored structures. The approach is also applicable for situations where  
436 several model-free methods are used for data interpretation. The methodology may uncover  
437 solutions that would not have been found using engineering judgement alone.
- 438 • When using several data-interpretation methods for damage identification, measurement  
439 systems should be configured by optimizing simultaneously all their objective functions

440 rather than using the union of best compromise measurement locations that are separately  
441 identified for each method.

- 442 • The number of non-detectable scenarios, the damage detectability and the average time to  
443 detection are useful metrics for configuring measurement systems when moving principal  
444 component analysis (MPCA) and robust regression analysis (RRA) are used for data  
445 interpretation.
- 446 • Damage scenario generation and multi-objective optimization of key metrics are helpful for  
447 measurement system configuration when data is interpreted using model-free methods.
- 448 • Multi-criteria decision-making (MCDM) methods such as Preference Ranking Organization  
449 METHod for Enrichment Evaluation (PROMETHEE) and Pareto-Edgeworth-MCDM (PEG-  
450 MCDM) can provide support for selecting the best compromise measurement-system  
451 configuration.

452 Future work involves a development of a model-free data-interpretation approach that combines  
453 MPCA and RRA methods. Taking into account thermal response for improving structural  
454 identification is another current research topic.

## 455 **Acknowledgements**

456 This work was funded by Swiss National Science Foundation under contract no. 200020-126385. The  
457 authors would like to thank A. Nussbaumer for his contributions related to the case study.

## 458 **References**

- 459 Andersen, R. (2008). *Modern methods for robust regression*, SAGE Publications, Inc.
- 460 Aref, A. J., Alampalli, S., and He, Y. (2005). "Performance of a fiber reinforced polymer web core skew bridge  
461 superstructure. Part I: field testing and finite element simulations." *Composite Structures*, 69(4), 491-499.
- 462 ASCE. (2011). "Structural Identification of Constructed Facilities." Structural Identification Committee, American  
463 Society of Civil Engineers.
- 464 Behzadian, M., Kazemzadeh, R. B., Albadvi, A., and Aghdasi, M. (2010). "PROMETHEE: A comprehensive  
465 literature review on methodologies and applications." *European Journal of Operational Research*, 200(1),  
466 198-215.
- 467 Bel Hadj Ali, N., and Smith, I. F. C. (2010). "Dynamic behavior and vibration control of a tensegrity structure."  
468 *International Journal of Solids and Structures*, 47(9), 1285-1296.

469 Brans, J.-P., and Mareschal, B. (2005a). "Promethee Methods." *Multiple Criteria Decision Analysis: State of the*  
470 *Art Surveys*, 163-186.

471 Brans, J. P. (1982). "L'ingénierie de la décision: élaboration d'instruments d'aide à la décision. La méthode  
472 PROMETHEE." *Laide a la Decision: Nature, Instrument s et Perspectives Davenir*, R. Nadeau and M. Landry,  
473 eds., Presses de l'Université Laval, Quebec. Canada, 183-214.

474 Brans, J. P., and Mareschal, B. (2005b). "Promethee Methods." *Multiple Criteria Decision Analysis: State of the*  
475 *Art Surveys*, 163-186.

476 Brans, J. P., Vincke, P., and Mareschal, B. (1986). "How to select and how to rank projects: The Promethee  
477 method." *European Journal of Operational Research*, 24(2), 228-238.

478 Cha, Y.-J., Raich, A., Barroso, L., and Agrawal, A. (2011). "Optimal placement of active control devices and  
479 sensors in frame structures using multi-objective genetic algorithms." *Structural Control and Health*  
480 *Monitoring*.

481 Chen, S. R., and Wu, J. (2010). "Dynamic Performance Simulation of Long-Span Bridge under Combined Loads of  
482 Stochastic Traffic and Wind." *Journal of Bridge Engineering*, 15(3), 219-230.

483 Coello Coello, C. A., Lamont, G. B., and Van Veldhuizen, D. A. (2007). *Evolutionary Algorithms for Solving Multi-*  
484 *Objective Problems*, Springer US.

485 Fleming, P. J., Purshouse, R. C., and Lygoe, R. J. (2005). "Many-Objective Optimization: An Engineering Design  
486 Perspective." *Evolutionary Multi-Criterion Optimization*, 14-32.

487 Goulet, J.-A., Kripakaran, P., and Smith, I. F. C. (2010). "Multimodel Structural Performance Monitoring."  
488 *Journal of Structural Engineering*, 136(10), 1309-1318.

489 Grierson, D. E. (2008). "Pareto multi-criteria decision making." *Advanced Engineering Informatics*, 22(3), 371-  
490 384.

491 Hou, Z., Noori, M., and St. Amand, R. (2000). "Wavelet-based approach for structural damage detection."  
492 *Journal of Engineering Mechanics*, 126(7), 677-683.

493 Hubert, M., Rousseeuw, P. J., and Branden, K. V. (2005). "ROBPCA: A new approach to robust principal  
494 component analysis." *Technometrics*, 47, 64-79.

495 Jaishi, B., and Ren, W.-X. (2006). "Damage detection by finite element model updating using modal flexibility  
496 residual." *Journal of Sound and Vibration*, 290(1-2), 369-387.

497 Jajo, N. (2005). "A Review of Robust Regression and Diagnostic Procedures in Linear Regression." *Acta*  
498 *Mathematicae Applicatae Sinica (English Series)*, 21(2), 209-224.

499 Kang, F., Li, J.-j., and Xu, Q. (2008). "Virus coevolution partheno-genetic algorithms for optimal sensor  
500 placement." *Advanced Engineering Informatics*, 22(3), 362-370.

501 Koh, C. G., and Thanh, T. N. (2009). "Challenges and Strategies in Using Genetic Algorithms for Structural  
502 Identification." *Soft Computing in Civil and Structural Engineering*, B. H. V. Topping and Y. Tsompanakis,  
503 eds., Saxe-Coburg Publications, Stirlingshire, UK, 203-226.

504 Kripakaran, P., and Smith, I. F. C. (2009). "Configuring and enhancing measurement systems for damage  
505 identification." *Advanced Engineering Informatics*, 23(4), 424-432.

506 Lanata, F., and Grosso, A. D. (2006). "Damage detection and localization for continuous static monitoring of  
507 structures using a proper orthogonal decomposition of signals." *Smart Materials and Structures*, 15(6),  
508 1811-1829.

509 Li, D. S., Li, H. N., and Fritzen, C. P. (2007). "The connection between effective independence and modal kinetic  
510 energy methods for sensor placement." *Journal of Sound and Vibration*, 305(4-5), 945-955.

511 Li, Z. N., Tang, J., and Li, Q. S. (2004). "Optimal sensor locations for structural vibration measurements." *Applied*  
512 *Acoustics*, 65(8), 807-818.

513 Liu, M., Frangopol, D. M., and Kim, S. (2009). "Bridge Safety Evaluation Based on Monitored Live Load Effects."  
514 *Journal of Bridge Engineering*, 14(4), 257-269.

515 Liu, W., Gao, W.-c., Sun, Y., and Xu, M.-j. (2008). "Optimal sensor placement for spatial lattice structure based  
516 on genetic algorithms." *Journal of Sound and Vibration*, 317(1-2), 175-189.

517 Meo, M., and Zumpano, G. (2005). "On the optimal sensor placement techniques for a bridge structure."  
518 *Engineering Structures*, 27(10), 1488-1497.

519 Ni, Y. Q., Zhou, H. F., Chan, K. C., and Ko, J. M. (2008). "Modal Flexibility Analysis of Cable-Stayed Ting Kau  
520 Bridge for Damage Identification." *Computer-Aided Civil and Infrastructure Engineering*, 23(3), 223-236.

521 Omenzetter, P., and Brownjohn, J. M. W. (2006). "Application of time series analysis for bridge monitoring."  
522 *Smart Materials and Structures*, 15(1), 129-138.

523 Papadimitriou, C. (2004). "Optimal sensor placement methodology for parametric identification of structural  
524 systems." *Journal of Sound and Vibration*, 278(4-5), 923-947.

525 Posenato, D., Kripakaran, P., Inaudi, D., and Smith, I. F. C. (2010). "Methodologies for model-free data  
526 interpretation of civil engineering structures." *Computers & Structures*, 88(7-8), 467-482.

527 Posenato, D., Lanata, F., Inaudi, D., and Smith, I. F. C. (2008). "Model-free data interpretation for continuous  
528 monitoring of complex structures." *Advanced Engineering Informatics*, 22(1), 135-144.

529 Rakesh, K. K., and et al. (2008). "Placement Optimization of Distributed-Sensing Fiber-Optic Sensors Using  
530 Genetic Algorithms." *AIAA Journal*, 46(4), 824.

531 Rao, A. R. M., and Ganesh, A. (2007). "Optimal placement of sensors for structural system identification and  
532 health monitoring using a hybrid swarm intelligence technique." *Smart Materials and Structures*, 16(6),  
533 2658.

534 Raphael, B., and Smith, I. F. C. (2003). "A direct stochastic algorithm for global search." *Applied Mathematics  
535 and Computation*, 146(2-3), 729-758.

536 Robert-Nicoud, Y., Raphael, B., Burdet, O., and Smith, I. F. C. (2005a). "Model Identification of Bridges Using  
537 Measurement Data." *Computer-Aided Civil and Infrastructure Engineering*, 20(2), 118-131.

538 Robert-Nicoud, Y., Raphael, B., and Smith, I. F. C. (2005b). "Configuration of measurement systems using  
539 Shannon's entropy function." *Computers and structures*, 83(8-9), 599-612.

540 Saitta, S., Raphael, B., and Smith, I. F. C. (2005). "Data mining techniques for improving the reliability of system  
541 identification." *Advanced Engineering Informatics*, 19(4), 289-298.

542 Saitta, S., Raphael, B., and Smith, I. F. C. (2006). "Rational Design of Measurement Systems using Information  
543 Science." *IABSE Symposium Report*, 92(25), 37-44.

544 Sastry, K. (2007). "Single and Multiobjective Genetic Algorithm Toolbox for Matlab in C++ (IlligAL Report No.  
545 2007017)." IL: University of Illinois at Urbana-Champaign, Urbana, USA.

546 Tongpadungrod, P., Rhys, T. D. L., and Brett, P. N. (2003). "An approach to optimise the critical sensor locations  
547 in one-dimensional novel distributive tactile surface to maximise performance." *Sensors and Actuators A:  
548 Physical*, 105(1), 47-54.

549 Wang, H., Song, Z., and Wang, H. (2002). "Statistical process monitoring using improved PCA with optimized  
550 sensor locations." *Journal of Process Control*, 12(6), 735-744.

551 Xu, J., Johnson, M. P., Fischbeck, P. S., Small, M. J., and VanBriesen, J. M. (2010). "Robust placement of sensors  
552 in dynamic water distribution systems." *European Journal of Operational Research*, 202(3), 707-716.

553 Yan, A. M., Kerschen, G., De Boe, P., and Golinval, J. C. (2005). "Structural damage diagnosis under varying  
554 environmental conditions--part II: local PCA for non-linear cases." *Mechanical Systems and Signal  
555 Processing*, 19(4), 865-880.

556

557

558

**Table 1. Estimated execution times for single and multi-objective optimization**

Search algorithm	Number of evaluations	Estimated execution time
Single objective	400	0.6 hour
Three objectives	40000	60 hours
Five objectives	4000000	6000 hours

**Table 2. Properties of truss members of a railway bridge in Zangenberg, Germany**

Member type	Area (m <sup>2</sup> )	I <sub>x</sub> (m <sup>4</sup> )	I <sub>y</sub> (m <sup>4</sup> )	Length (m)
Top chord	5.15 x 10 <sup>-2</sup>	2.27 x 10 <sup>-3</sup>	2.58 x 10 <sup>-3</sup>	4.00
Bottom chord	3.03 x 10 <sup>-1</sup>	1.47 x 10 <sup>-3</sup>	1.46 x 10 <sup>-3</sup>	2.00
Vertical	2.19 x 10 <sup>-2</sup>	1.21 x 10 <sup>-3</sup>	4.24 x 10 <sup>-5</sup>	4.00
Diagonal	3.69 x 10 <sup>-2</sup>	9.70 x 10 <sup>-4</sup>	4.16 x 10 <sup>-3</sup>	5.66
Small diagonal	2.19 x 10 <sup>-2</sup>	1.21 x 10 <sup>-3</sup>	4.24 x 10 <sup>-5</sup>	5.66

**Table 3. Outranking solutions of the Pareto-optimum set for MPCA**

Rank	$\varphi$	PROMETHEE (Configuration number)	Distance	PEG-MCDM (Configuration number)
1	9.3	8	4.8E-03	7
2	9.1	13	6.1E-03	8
3	8.5	7	1.0E-02	4
4	7.4	5	1.1E-02	5
5	6.9	4	1.8E-02	11

**Table 4. Outranking solutions of the Pareto-optimum set for RRA**

Rank	$\varphi$	PROMETHEE (Configuration number)	Distance	PEG-MCDM (Configuration number)
1	9.8	16	9.9E-03	13
2	5.1	19	1.1E-02	16
3	3.4	18	1.5E-02	9
4	3.0	13	1.6E-02	12
5	1.9	4	1.7E-01	18

**Table 5. Performance of the optimum configuration for different data-interpretation methods. Criteria 1 is the number of non-detectable damage scenarios; Criteria 2 is the damage detectability (%); and Criteria 3 is the average time to detection (days).**

Data-interpretation method	Number of sensors	Criteria 1	Criteria 2	Criteria 3
MPCA	24	17	86.2	139.5
RRA	24	42	45.0	3.0
Union of MPCA and RRA	38	17	86.3	47.4
Optimized combination of MPCA and RRA	24	13	92.5	87.6

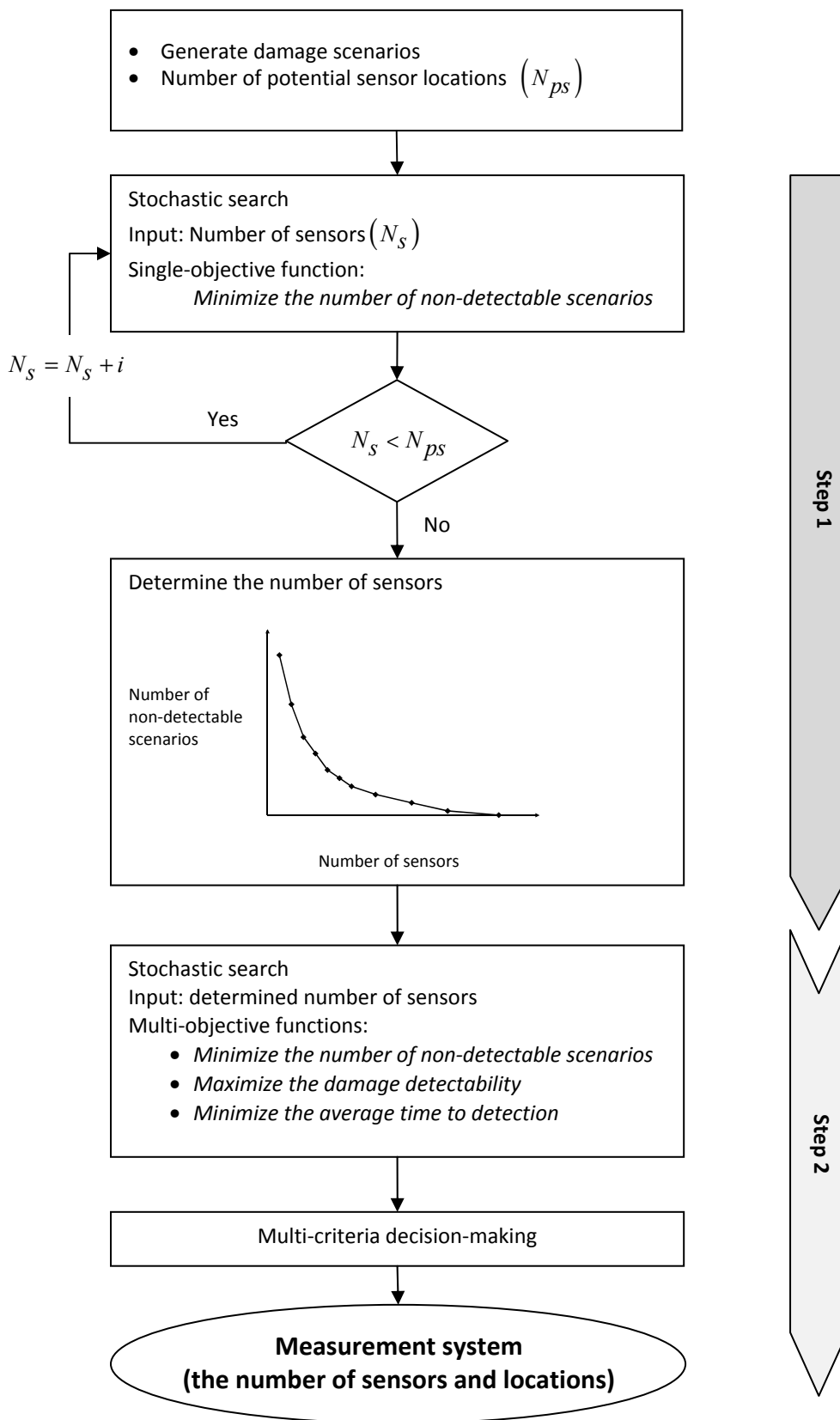
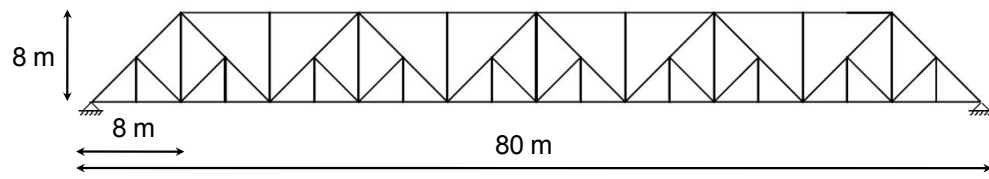
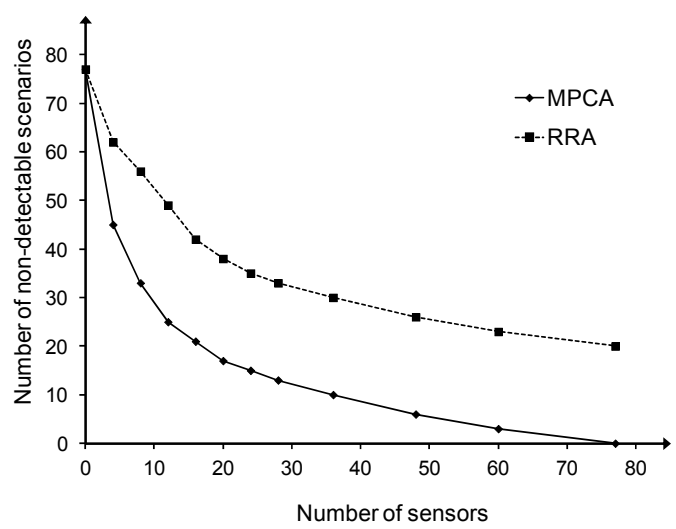


Figure 1. A flowchart of a systematic approach for measurement-system configuration



**Figure 2. A truss structure inspired by a 80-m railway bridge**



**Figure 3. Number of non-detectable scenarios corresponding to the number of sensors**

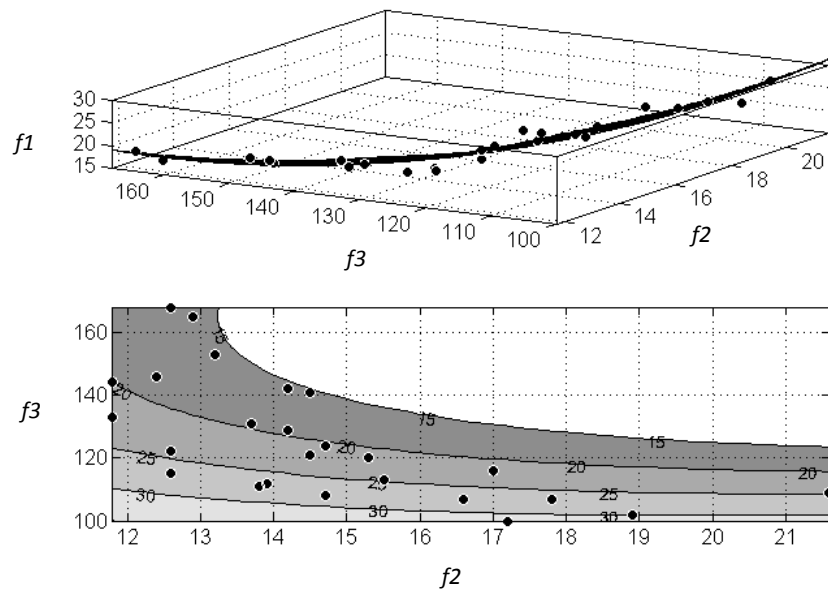


Figure 4. Pareto-optimal solutions for MPCA.  $f1$  is the number of non-detectable damage scenarios;  $f2$  is the average minimum detectable damage-level (%); and  $f3$  is the average time to detection (days). The contour values in the lower figure refer to values of  $f1$ .

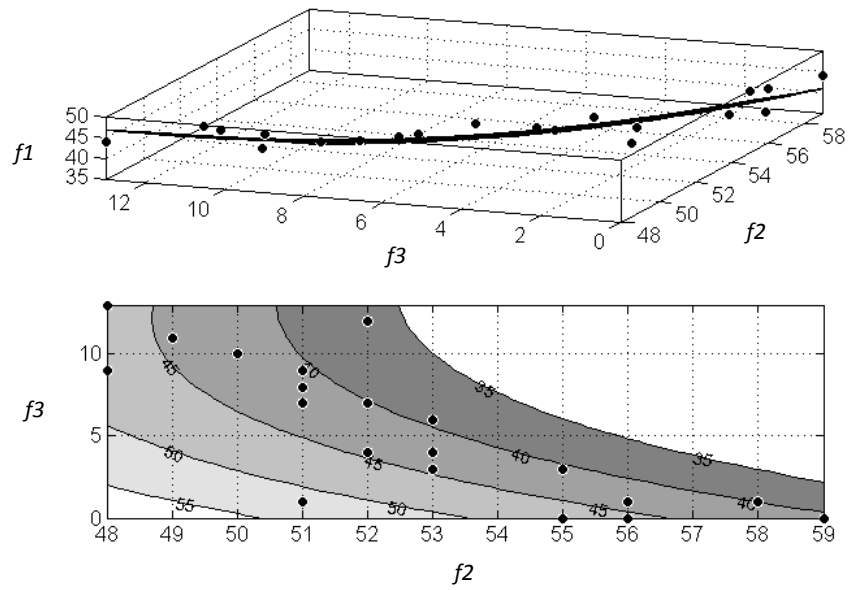
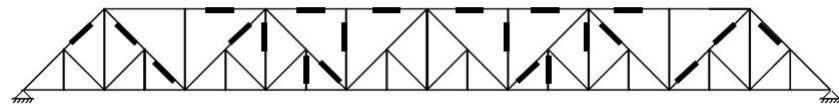
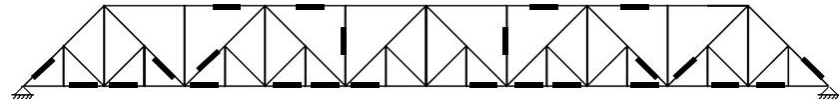


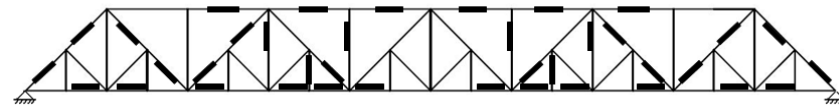
Figure 5 Pareto-optimal solutions for RRA.  $f_1$  is the number of non-detectable damage scenarios;  $f_2$  is the average minimum detectable damage-level (%); and  $f_3$  is the average time to detection (days). The contour values in the lower figure refer to values of  $f_1$ .



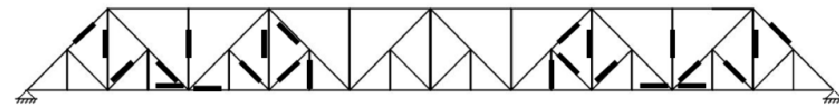
a) *Moving principal component analysis (MPCA)*



b) *Robust regression analysis (RRA)*



c) *Union of configurations (a) and (b)*



d) *Optimized combination of MPCA and RRA*

**Figure 6. Measurement system configuration for situations where (a) MPCA, (b) RRA, (c) union of a and b; and (d) optimized combination of MPCA and RRA are employed for data interpretation.**